

# Au–Cu Alloy Nanocluster Doped SiO<sub>2</sub> Films by Sol–Gel Processing

G. De,<sup>†</sup> G. Mattei,<sup>\*,‡</sup> P. Mazzoldi,<sup>‡</sup> C. Sada,<sup>‡</sup> G. Battaglin,<sup>§</sup> and A. Quaranta<sup>||</sup>

*Sol-Gel Division, Central Glass and Ceramic Research Institute, 196, Raja S.C. Mullick Road, Calcutta 700032, India; INFN, Dipartimento di Fisica, Università di Padova, via Marzolo 8, I-35131 Padova, Italy; INFN, Dipartimento di Chimica Fisica, Università di Venezia, Calle Larga Santa Marta 2137, 30123 Venezia, Italy; and INFN-Padova, Dipartimento di Ingegneria dei Materiali, Università di Trento, via Mesiano 77, I-38050 Trento, Italy*

*Received March 29, 2000. Revised Manuscript Received May 2, 2000*

Au–Cu alloy nanocluster formation in silica films has been achieved in the present study by sol–gel processing. A fundamental role for obtaining alloy clusters instead of separation of the metallic species is played by the annealing atmosphere. Annealing in reducing atmosphere (hydrogen-containing) results in Au–Cu alloy formation, whereas air annealing promotes not only Au cluster precipitation and Cu oxidation but also Au–Cu alloy separation in samples previously annealed under reducing atmosphere.

## Introduction

Composite materials formed by metal or semiconductor nanoclusters in insulating matrixes have been the object of continuously growing interest in the fields of colloid science and nonlinear optical properties of colloids.<sup>1,2</sup> The formation of two types of clusters, mixed composition clusters or alloy clusters,<sup>3–8</sup> in the same matrix is peculiarly interesting from two points of view: the influence of the cluster composition or cluster interaction on either the optical absorption coefficient or on the composites nonlinear optical properties. Indeed the optical behavior of nanocluster composites (linear as well as nonlinear) is not only influenced by the cluster size and the volume fraction of the clusters but also by cluster distribution and composition. In a previous paper,<sup>9</sup> we explored the possibility of controlling the optical properties of sol–gel-derived Ag nanocluster doped films in mixed ZrO<sub>2</sub>–SiO<sub>2</sub> matrixes with different relative composition and therefore different refractive indices. Moreover, the optical properties of thin silica

films, containing Ag and Cu clusters, prepared by the sol–gel technique, have been studied in refs 4–6. Separated Ag and Cu nanoclusters<sup>4–6</sup> or under particular experimental conditions mixed Ag–Cu clusters made up of both Ag and Cu<sup>5</sup> were evidenced and the presence of both cluster species affected the optical properties of the films. On the contrary, Ag–Cu,<sup>3</sup> Au–Cu,<sup>8</sup> and Ag–Au<sup>10</sup> alloy clusters were reported by ion implantation. A few papers appeared in the literature concerning the formation of metallic alloy nanoclusters via the sol–gel route, mostly involving transition metals for magnetic applications: Nd–Fe,<sup>11</sup> Fe–Cr,<sup>12</sup> Fe–Ni,<sup>13,14</sup> Cu–Ni,<sup>15</sup> and Fe–Co.<sup>16</sup>

In this paper we present a study of the structural and optical properties of silica films, containing Au and Cu, prepared by sol–gel processing. An important aim is to individuate the influence of annealing atmosphere on the formation of Au–Cu alloy or separated Au and Cu systems, by using the selective influence on the Au and Cu precipitation in hydrogen and/or oxygen (air) annealing atmospheres.

## Experimental Section

Film compositions (in moles) are given in Table 1. The Au–Cu codoped silica films were prepared by the sol–gel dip-coating technique from sols prepared from Si(OC<sub>2</sub>H<sub>5</sub>)<sub>4</sub> (TEOS), HAuCl<sub>4</sub>·3H<sub>2</sub>O, CuCl<sub>2</sub>·2H<sub>2</sub>O, a catalytic amount of HCl, H<sub>2</sub>O, *n*-propyl alcohol, and isobutyl alcohol. The film composition [i.e. the molar ratio of total metal (Au + Cu) and SiO<sub>2</sub>] is kept

\* Corresponding author. Fax: +39.049.8277003. E-mail: mattei@padova.infn.it.

<sup>†</sup> Central Glass and Ceramic Research Institute.

<sup>‡</sup> Università di Padova.

<sup>§</sup> Università di Venezia.

<sup>||</sup> Università di Trento.

(1) Mazzoldi, P.; Arnold, G. W.; Battaglin, G.; Gonella, F.; Haglund, R. F., Jr. *J. Nonlinear Opt. Phys. Mater.* **1996**, *5*, 285.

(2) Gonella, F.; Mazzoldi, P. Metal Nanocluster Composite Glasses. In *Handbook of Nanostructured Materials and Nanotechnology*; Nalwa, H. S., Ed.; Academic Press: San Diego, 2000; Vol. 4, pp 81–158.

(3) Magruder, R. H., III; Osborne, D. H., Jr.; Zuh, R. A. *J. Non-Cryst. Solids* **1994**, *176*, 299.

(4) De, G.; Tapfer, L.; Catalano, M.; Battaglin, G.; Caccavale, F.; Gonella, F.; Mazzoldi, P.; Haglund, R. F., Jr. *Appl. Phys. Lett.* **1996**, *68*, 3820.

(5) De, G.; Gusso, M.; Tapfer, L.; Catalano, M.; Gonella, F.; Mattei, G.; Mazzoldi, P.; Battaglin, G. *J. Appl. Phys.* **1996**, *80*, 6734.

(6) Catalano, M.; Carlino, E.; De, G.; Tapfer, L.; Gonella, F.; Mazzoldi, P.; Battaglin, G. *Philos. Mag. B* **1997**, *76*, 621.

(7) Yasuda, H.; Mori, H. *Z. Phys. D* **1994**, *31*, 131.

(8) Gonella, F.; Mattei, G.; Mazzoldi, P.; Sada, C.; Battaglin, G.; Cattaruzza, E. *Appl. Phys. Lett.* **1999**, *75*, 55.

(9) Gonella, F.; Mattei, G.; Mazzoldi, P.; Battaglin, G.; Quaranta, A.; De, G.; Montecchi, M. *Chem. Mater.* **1999**, *11*, 814.

(10) Battaglin, G.; Cattaruzza, E.; Gonella, F.; Mattei, G.; Mazzoldi, P.; Sada, C.; Zhang, X. *Nucl. Instr. Methods B* **2000**, *166*, 857.

(11) Lin, J.; Liu, S.; Qian, X.; Bayi, J.; Su, M. *J. Alloys Compd.* **1996**, *238*, 113.

(12) Chatterjee, A.; Das, D.; Chakravorty, D.; Choudhury, K. *Appl. Phys. Lett.* **1990**, *57*, 1360.

(13) Wang, J.-P.; Han, D.-H.; Luo, H.-L.; Gao, N.-F.; Liu, Y.-Y. *J. Magn. Magn. Mater.* **1994**, *135*, L251.

(14) Leslie-Pelecky, D. L.; Rieke, R. D. *Chem. Mater.* **1996**, *8*, 1770.

(15) Kaiser, A.; Gorsmann, C.; Schubert, U. *J. Sol-Gel Sci. Technol.* **1997**, *8*, 795.

(16) Hou, D. L.; Tang, G. D.; Chen, W.; Liu, Y.; Nie, X. F.; Luo, H. L. *Phys. Status Solidi A* **1998**, *169*, 131.

**Table 1. Nominal and Measured (by RBS) Compositions of Mixed Au–Cu Nanocluster Doped SiO<sub>2</sub> Films Annealed at 800 °C in H<sub>2</sub>–N<sub>2</sub> Atmosphere**

| sample  | film thickness (nm) | nominal composition (mol Au:mol Cu:mol Si) | Cu/Au molar ratio (nominal) | composition by RBS (mol Au:mol Cu:mol Si) | Cu/Au molar ratio (RBS) |
|---------|---------------------|--------------------------------------------|-----------------------------|-------------------------------------------|-------------------------|
| 1Au2CuH | 90                  | 5:10:85                                    | 2.0                         | 4.7:9:86.3                                | 1.9                     |
| 1Au6CuH | 95                  | 2.1:12.9:85                                | 6.0                         | 1.6:11:87.4                               | 6.8                     |
| 1Au8CuH | 120                 | 1.67:13.3:85                               | 8.0                         | 1.5:12.5:86.0                             | 8.3                     |

constant in all the Au–Cu codoped films, being 15 equivalent mol % (Au + Cu) – 85% SiO<sub>2</sub>. The films named as 1Au2Cu (5 mol % Au–10 mol % Cu), 1Au6Cu (2.1 mol % Au–12.9 mol % Cu), and 1Au8Cu (1.67 mol %–13.33 mol % Cu) were prepared. The general preparation method of these films is as follows: the required amount of TEOS is first dissolved in *n*-propyl alcohol (50% of total amount). To this, first CuCl<sub>2</sub>·2H<sub>2</sub>O solution (dissolved in 50% of the total H<sub>2</sub>O) followed by an aqueous solution of HAuCl<sub>4</sub>·3H<sub>2</sub>O was added with stirring. A residual amount of *n*-propyl alcohol was then added and the solution was stirred for 30 min. After this period isobutyl alcohol was added and the sol stirred for another 1 h. The total H<sub>2</sub>O/TEOS and HCl/TEOS molar ratios were 8 and 0.01, respectively. The total equivalent oxide (including dopants) content of the sols was about 4.5 wt % in all cases. The film thickness was measured by RBS and it was found to vary in the range 90–120 nm. Thoroughly cleaned silica glasses (type II, Heraeus) were used as substrates. For the dip-coating preparation, a withdrawal velocity of 1.67 mm/s was maintained. The resulting films were first dried at 60 °C in air then heat-treated to 500–800 °C in air to obtain mixed Au/Cu oxide films. In the air-baked (500 °C) codoped films, when annealed in an 8% H<sub>2</sub>–92% N<sub>2</sub> gas atmosphere, were obtained alloy Au–Cu nanoclusters doped films. The samples are labeled as 1AumCuX, where *m* is the [Cu]/[Au] molar ratio, and *X* indicates the type of annealing, i.e., *X* = A, H, HA, for annealing in air, in 8% H<sub>2</sub>–92% N<sub>2</sub> and sequential annealing in 8% H<sub>2</sub>–92% N<sub>2</sub> and air, respectively.

The gold, copper, silicon, and oxygen profiles in the films were determined by Rutherford backscattering spectrometry (RBS). A <sup>4</sup>He<sup>+</sup> beam at the energy of 2.2 MeV was used at National Laboratories INFN-Legnano. Optical absorption spectra were determined in the wavelength region from 200 to 800 nm, by using a Cary UV–Vis–NIR dual-beam spectrophotometer. Samples for transmission electron microscopy (TEM) were prepared by cutting 3 mm diameter disks from the samples with a slurry drill and mechanically grinding the disks from the backside to a thickness of about 20 μm. The final thinning to electron transparency was achieved by planar back-thinning by ion milling with an Ar gun at 5 keV. Samples were cryogenically cooled during ion milling. The prepared samples were examined at the CNR-LAMEL Institute Bologna, with a Philips CM30 TEM operating at 300 kV and equipped with an EDAX energy-dispersive X-ray spectrometer (EDS) for compositional analysis.

## Results and Discussion

The coating films were first dried at 60 °C and heat-treated at 500 °C for 30 min to remove the organic matters. The resultant films were reddish purple in color due to the formation of Au metal nanoclusters through the decomposition of Au salts at 500 °C. These 500 °C heat-treated films were further heated in air (oxidizing) and 8% H<sub>2</sub>–92% N<sub>2</sub> (reducing) atmospheres.

The three sets of coatings corresponding to the Cu/Au molar ratios of 2, 6, and 8 were analyzed by a Rutherford backscattering (RBS) technique to check the compositions. The results (Table 1) were in good agreement with their nominal compositions.

**3.1. Optical Absorption.** The optical spectra of the 1Au2Cu films heated for 1 h in H<sub>2</sub>–N<sub>2</sub> (sample 1Au2CuH) and air atmosphere (1Au2CuA), respectively, are shown in Figure 1. The film heated in H<sub>2</sub>–N<sub>2</sub> (curve

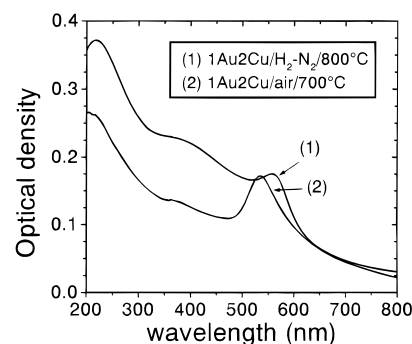


**Figure 1.** Optical absorption spectra of 1Au2Cu films annealed in H<sub>2</sub>–N<sub>2</sub> and air atmospheres. Film thickness was 90 nm. Both sides of the substrate were coated.

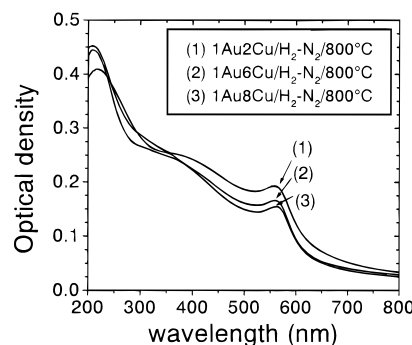


**Figure 2.** Optical absorption spectra of 1Au2Cu, 1Au6Cu, and 1Au8Cu films annealed in H<sub>2</sub>–N<sub>2</sub> atmosphere at 800 °C for 1 h. The film thickness was normalized to 100 nm in all cases.

1) exhibits a surface plasmon resonance (SPR) peak at 553 nm, which is between that of pure Au cluster in SiO<sub>2</sub> (located at ~530 nm) and that of pure Cu (~570 nm). This suggests the formation of Au–Cu alloy nanoclusters as in ref 8. The corresponding air-baked (700 °C) film shows a SPR peak at 535 nm (curve 2) due to the presence of Au nanoclusters only<sup>1</sup> because it is not possible to reduce the Cu<sup>2+</sup> ions in air (oxidation atmosphere). Therefore, in this film copper remained an oxide. It may also be noted that when 1Au6Cu and 1Au8Cu samples were heated in air at 800 °C results similar to those of 1Au2Cu sample were obtained. In these cases also only an Au SPR peak at 525 nm was observed. As copper remained as copper oxide in the air-baked films, no interband transition peak near 215 nm due to Cu<sup>17,18</sup> was observed in their absorption spectra.

Figure 2 shows the optical absorption curves of 1Au2Cu, 1Au6Cu, and 1Au8Cu films heated at 800 °C in an H<sub>2</sub>–N<sub>2</sub> atmosphere. In all the cases Au–Cu alloy clusters were formed, as evidenced by the SPR peak in the 553–563 nm range. A slight red shifting (toward the SPR of pure Cu nanocluster) of the Au–Cu alloy SPR positions was noticed due to the increase of Cu

(17) Anderson, A. B. *J. Chem. Phys.* **1978**, *68*, 1744.

(18) Creighton, J. A.; Eadon, D. G. *J. Chem. Soc., Faraday Trans.* **1991**, *87*, 3881.

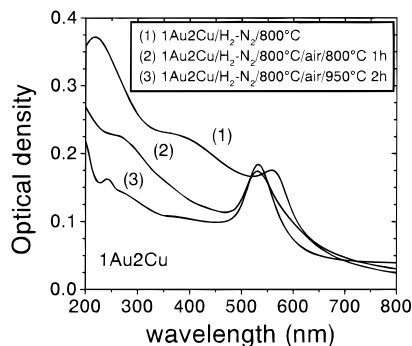


**Figure 3.** Optical absorption spectra showing the decomposition of 1Au2Cu alloy structure after heat treatment in air at 800 °C for 1 h and 950 °C for 2 h. Film thickness was 90 nm.

concentration in the alloy (in cases of 1Au2CuH at 553 nm, 1Au6CuH at 560 nm, and 1Au8CuH at 563 nm, respectively). When these Au–Cu alloy cluster containing films are heated again in air, the alloy decomposes into metallic Au clusters and Cu oxide. Accordingly, the surface plasmon resonance of pure Au is visible at 532–535 nm. Figure 3 shows the decomposition of the Au–Cu alloy structure of the 1Au2CuH films when further heated in air at 800 °C for 1 h and at 950 °C for 2 h (1Au2CuHA). At 800 °C, the SPR of Au nanocluster was observed at 535 nm along with an absorption shoulder at 250–270 nm due to the presence of Cu in oxidized form,<sup>5,19</sup> which disappeared at 950 °C, due to the evaporation of copper from the matrix. As a result, the absorption spectrum of the 950 °C heated sample (Figure 3) resembles that of pure Au nanocluster doped silica films.<sup>20,21</sup>

**3.2. TEM.** The picture of Au–Cu alloy formation in the samples annealed in H<sub>2</sub>–N<sub>2</sub> has been confirmed by TEM analysis. Selected area electron diffraction (SAED) on the sample 1Au6Cu annealed in H<sub>2</sub>–N<sub>2</sub> (1Au6CuH) exhibits Debye–Scherrer rings that can be ascribed to a fcc phase with lattice parameter  $a = 0.369 \pm 0.002$  nm. Similar results are obtained for the 1Au2Cu sample annealed under the same conditions (1Au2CuH): in this case, the fcc phase has a lattice parameter  $a = 0.381 \pm 0.002$  nm. Both these values differ from those of the fcc bulk phase of pure Au or pure Cu, which have lattice parameters  $a_{\text{Au}} = 0.40786$  nm and  $a_{\text{Cu}} = 0.36150$  nm, respectively. This confirms the formation of Au–Cu alloy clusters in the case of annealing in H<sub>2</sub>–N<sub>2</sub> atmosphere. In the air-annealed samples (1Au2CuA and 1Au6CuA), on the contrary, we obtained a fcc phase with  $a = 0.407 \pm 0.002$  nm, which indicates that Au and Cu do not form an alloy but remain separated and Au precipitates in clusters, while Cu is oxidized. This holds also for the 1Au2Cu sample annealed first in H<sub>2</sub>–N<sub>2</sub> at 800 °C (sample 1Au2CuH, with alloy formation) and then in air at 800 or 950 °C (1Au2CuHA): this implies that air annealing is able to decompose the already formed alloy (due to Cu–O interaction), as also evidenced in the optical absorption spectra of Figure 3. In Figure 4a we report the radially averaged (SAED pattern) intensity of the samples 1Au2Cu and 1Au6Cu annealed in H<sub>2</sub>–N<sub>2</sub> at 800 °C for 1 h (samples 1Au2CuH and 1Au6CuH, respectively).

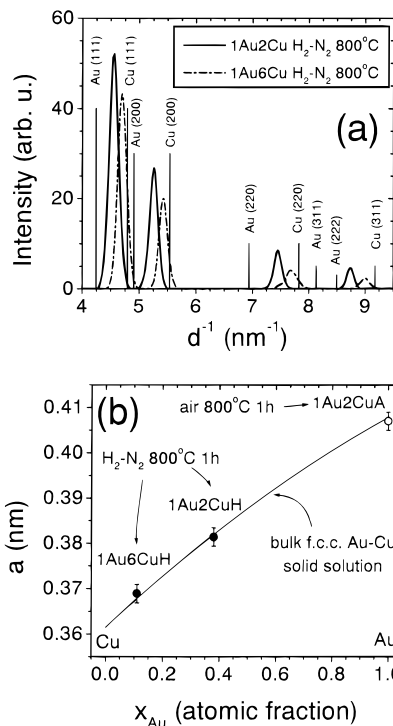


**Figure 4.** (a) Radially averaged intensity of the selected area electron diffraction pattern in the 1Au2Cu and 1Au6Cu samples annealed in H<sub>2</sub>–N<sub>2</sub> at 800 °C for 1 h (samples 1Au2CuH and 1Au6CuH, respectively). The patterns can be indexed in both cases with a fcc phase. For comparison, the diffraction peak positions of the fcc phase of pure Au and Cu are reported. (b) Measured lattice parameters in the 1Au2Cu and 1Au6Cu samples annealed in H<sub>2</sub>–N<sub>2</sub> at 800 °C for 1 h (filled circles, samples 1Au2CuH and 1Au6CuH, respectively) and 1Au2Cu annealed in air at 800 °C for 1 h (open circle, sample 1Au2CuA). For comparison, the modified Vegard's law (solid line) representing the evolution of the lattice parameter in the bulk fcc intermetallic alloy is reported.

and 1Au6CuH); for comparison, the diffraction peak positions of the pure bulk Au and Cu fcc phases are reported. From EDS compositional analysis on single clusters we obtained an average atomic ratio  $\alpha = [\text{Cu}]/[\text{Au}]$  which is 1.6 and 6.5 for the 1Au2CuH and 1Au6CuH, respectively. These are smaller than the molar ratios found by RBS analysis (1.9 and 6.8, respectively), suggesting that some Cu remained in the silica glass. Indeed, EDS on that samples showed the presence of Cu in the matrix surrounding the clusters, probably in an oxidized form (Cu–O–Si, for instance). The values of the measured lattice parameters of hydrogen- and air-annealed samples are reported in Figure 4b, along with a curve representing, for comparison, the evolution of the lattice constant of the Au–Cu fcc solid solution,<sup>8</sup> according to a modified Vegard's law

$$a_{\text{alloy}} = xa_{\text{Au}} + (1 - x)a_{\text{Cu}} + 0.01198x(1 - x) \quad (1)$$

where  $x$  is the Au fraction in the intermetallic alloy.

All TEM results are summarized in Table 2, which reports the cluster composition obtained by EDS, the lattice parameter of the fcc nanostructures, and the size distribution (average diameter and standard deviation) of the clusters in the samples examined.

It is interesting to note that, in the case of sequentially Au–Cu implanted silica,<sup>8</sup> the annealing under

(19) Debnath, R.; Das, S. K. *Chem. Phys. Lett.* **1989**, *155*, 52.

(20) Matsuoka, J.; Mizutami, R.; Nasu, H.; Kamiya, K. *J. Ceram. Soc. Jpn.* **1992**, *100*, 599.

(21) Kozuka, H.; Sakka, S. *Chem. Mater.* **1993**, *5*, 222.



**Table 2. TEM Results on Mixed Au–Cu Nanocluster Doped SiO<sub>2</sub> Films Annealed at 800 °C in Different Atmospheres**

| sample   | annealing conditions                                         | [Cu]/[Au] on clusters (EDS) | <i>a</i> (nm) (SAED) | diameter (nm) (BF) |
|----------|--------------------------------------------------------------|-----------------------------|----------------------|--------------------|
| 1Au2CuH  | H <sub>2</sub> –N <sub>2</sub> 800 °C, 1 h                   | 1.6                         | 0.381 ± 0.002        | 12.5 ± 5.4         |
| 1Au2CuA  | air 800 °C, 1 h                                              | 0 (pure Au)                 | 0.407 ± 0.002        | 21 ± 10            |
| 1Au2CuHA | H <sub>2</sub> –N <sub>2</sub> 800 °C, 1 h + air 950 °C, 2 h | 0 (pure Au)                 | 0.407 ± 0.002        | 41 ± 15            |
| 1Au6CuH  | H <sub>2</sub> –N <sub>2</sub> 800 °C, 1 h                   | 6.5                         | 0.369 ± 0.002        | 6.2 ± 2.8          |

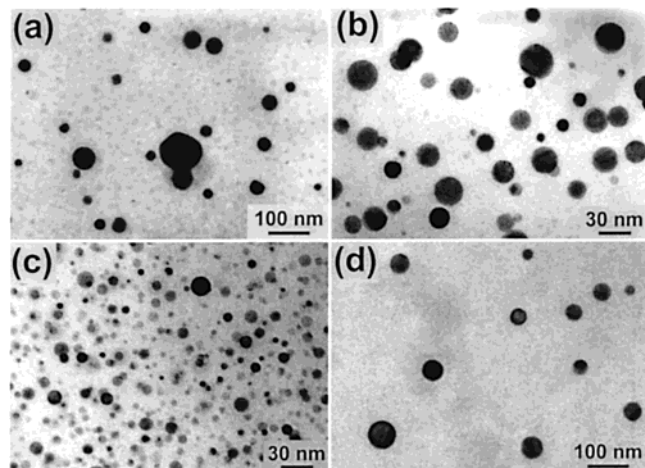


**Figure 5.** TEM bright-field planar view of the samples 1Au2Cu and 1Au6Cu annealed under different conditions: (a) 1Au2Cu at 800 °C in air for 1 h (1Au2CuA), (b) 1Au2Cu at 800 °C in H<sub>2</sub>–N<sub>2</sub> for 1 h (1Au2CuH), (c) 1Au6Cu at 800 °C in H<sub>2</sub>–N<sub>2</sub> for 1 h (1Au6CuH), (d) 1Au2Cu first at 800 °C in H<sub>2</sub>–N<sub>2</sub> for 1 h and then at 950 °C in air for 2 h (1Au2CuHA).

reducing atmosphere at 900 °C for 1 h resulted in a tetragonal ordered phase (tetra-aurocupride,  $a = 0.3960$  nm,  $c = 0.3670$  nm), which is the stable one below 400 °C for the bulk, according to the Au–Cu phase diagram near atomic fraction  $x = 0.5$ .<sup>22</sup> In the present study, only a fcc phase is obtained for all the compositions examined, probably due to the [Cu]/[Au] ratio, which is greater than unity in our samples. The TEM bright-field images of the samples 1Au2CuA, 1Au2CuH, 1Au6CuH, and 1Au2CuHA (see Table 2) are shown in Figure 5 and the corresponding size distribution histograms in Figure 6. Very large, spherical Au clusters with diameter  $\langle D \rangle = 21 \pm 10$  nm (average value and standard deviation) can be seen in the 1Au2CuA sample. Occasionally, faceted or twinned clusters have been found (Figure 5a). Samples 1Au2CuH and 1Au6CuH (parts b and c of Figure 5, respectively) exhibit spherical alloy cluster with  $\langle D \rangle = 12.5 \pm 5.4$  nm and  $\langle D \rangle = 6.2 \pm 2.8$  nm, showing that the relative Au and Cu concentration is an effective parameter that can be used not only to control the SPR position but also the size of the clusters. On performing a further air annealing at 950 °C for 2 h of the sample 1Au2CuH, a situation similar to the one of 1Au2CuA, i.e., very large and sparse clusters composed of pure Au, is obtained (sample 1Au2CuHA, Figure 5d). Such large clusters are due to a dissolution of the smaller ones, with subsequent oxygen-assisted gold diffusion and aggregation on the

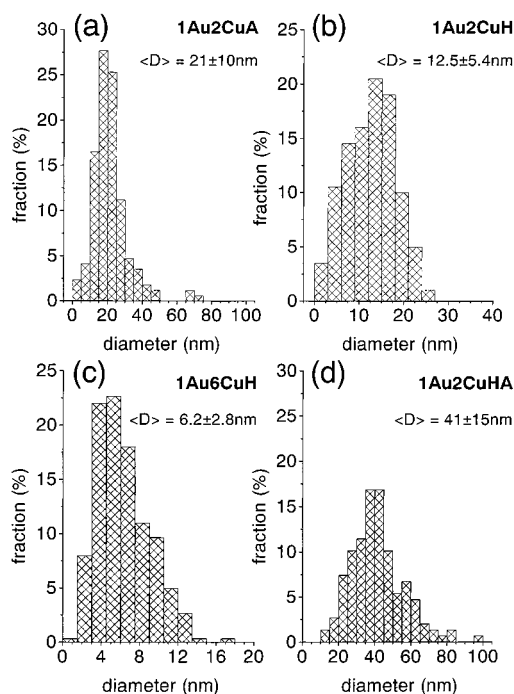


**Figure 6.** Histograms of size distribution of the samples reported in Figure 5: (a) 1Au2Cu at 800 °C in air for 1 h (1Au2CuA), (b) 1Au2Cu at 800 °C in H<sub>2</sub>–N<sub>2</sub> for 1 h (1Au2CuH), (c) 1Au6Cu at 800 °C in H<sub>2</sub>–N<sub>2</sub> for 1 h (1Au6CuH), (d) 1Au2Cu first at 800 °C in H<sub>2</sub>–N<sub>2</sub> for 1 h and then at 950 °C in air for 2 h (1Au2CuHA).

larger ones.<sup>10</sup> Moreover, EDS analysis on this sample evidenced a dramatic decrease of the total Cu concentration in the matrix, consistent with the evaporation of copper.

## Conclusions

In this work we demonstrated the possibility of producing by sol–gel processing alloy Au–Cu nanoclusters by using thermal annealing under reducing (hydrogen-containing) atmosphere with different relative Au:Cu ratios, size, and surface plasmon resonance positions. The structure of the alloy cluster is a fcc solid solution with lattice parameters in good agreement with the modified Vegard's law typical of bulk intermetallic Au–Cu alloy. The greater the Cu content in the alloy, the smaller the clusters size achieved. Subsequent annealing in oxidizing (air) atmosphere can be used to decompose the alloy clusters, separating Au (which forms metallic clusters) and Cu (which is oxidized).

**Acknowledgment.** This work has been partially supported by MURST (University and Research Ministry) within a National University Research Project. CM001053I

(22) Okamoto, H.; Chakrabarti, D. J.; Laughlin, D. E.; Massalski, T. B. In *Phase Diagrams of Binary Gold Alloys*; Monograph Series on Alloy Phase Diagrams; ASM Internationals: Metals Park, OH, 1987.